ISSN 1560-8034, 1605-6582 (On-line), SPQEO, 2019. V. 22, N 3. P. 277-284.

Key parameters of commercial silicon solar cells with rear metallization

A.V. Sachenko[1], V.P. Kostylyov[1], V.M. Vlasyuk[1], R.M. Korkishko[1], I.O. Sokolovskyi[1], V.V. Chernenko[1], B.F. Dvernikov[1], O.A. Serba[1], M.A. Evstigneev[2]

[1]V. Lashkaryov Institute of Semiconductor Physics, NAS of Ukraine
45, prospect Nauky, 03680 Kyiv, Ukraine
[2]Memorial University of Newfoundland, St. John's, NL, Canada
E-mail: sach@isp.kiev.ua; viktorvlasiuk@gmail.com

Abstract. The key parameters of silicon solar cells with back contact and rear metallization (SC-BC), such as the short-circuit current, open-circuit voltage, and photoconversion efficiency are modeled theoretically. Among other recombination channels, the model accounts for the non-radiative Auger recombination assisted by the deep recombination center and recombination in the space-charge region. It has been ascertained that these mechanisms are important in the typical commercial SC-BC in the maximal-power regime. The theory has been developed for calculating the efficiency as a function of the SC-BC thickness. Experimental and theoretical data agree well between each other. In particular, the theory has been applied to model the SC-BC produced by SunPower Corp. Depending on the surface recombination velocity on the illuminated surface and on the total surface recombination velocity on the front and rear surfaces, two mechanisms determine the optimal SC-BC thickness, at which the output power reaches its maximal. The first mechanism dominates, when the efficiency exceeds 24% under the AM1.5 conditions and is related to an essential increase of photon mean free path in the textured silicon SC. The other mechanism, more pronounced in the SC-BC with the efficiency below 22%, imposes limitations on the optimal thickness due to the surface recombination on the front SC-BC surface.

Keywords: solar cells, photoconversion efficiency, silicon, optimal thickness, surface recombination.

https://doi.org/10.15407/spqeo22.03.277
PACS 88.40.jj

Manuscript received 01.07.19; revised version received 15.07.19; accepted for publication 04.09.19; published online 16.09.19.

1. Introduction

In this work, the key parameters of commercial silicon solar cells with rear metallization (SC-BC) are modeled, with the emphasis on the ones produced by SunPower Corp. These SCs belong to the most efficient ones in the market, having the efficiency of about 22% [1-3]. The company SunPower Corp. was founded in 1985, and by 2001, it developed SCs with the collector junction and both contact electrodes located on the rear non-illuminated surface. Efficient solar panels were based on such SC-BC. Their efficiency gradually increased from 21.8% in 2006 to 22.5% in 2007, 23.3% in 2012, and in 2014 it was reported to reach 25% [1]. In 2016, the efficiency of the SC-BC based on an *n*-type Cz-silicon wafer with the thickness of 130 µm and the area 153.49 cm^2 reached the record value of 25.2% with the following other photoelectric parameters: open-circuit voltage V_{OC} = 737 mV, short-circuit current density J_{SC} = 41.33 mA/cm^2, fill factor FF = 82.7% [2]. The solar panels built on these SC-BC also have high efficiency, which is lower than the respective "parent" SC efficiency by less than 2.5%. In 2016, SunPower Corp. produced a solar panel with the efficiency of 24.1%, which consisted of 72 SC-BC with the efficiency of about 25% [2]. The mean efficiency of the solar panels presently produced by SunPower Corp. is 21.5% [3].

The one-dimensional theory developed here allows one to calculate the photoconversion efficiency η and other key parameters of SC-BC, such as the short-circuit current I_{SC}, open-circuit voltage V_{OC}, and the *I-V* curve fill factor FF. It is valid when the following criteria are fulfilled: (1) $L_d \gg d$, (2) $S_S \ll D_A/d$, where L_d is the electron-hole pair diffusion length, d – base thickness, S_S – total recombination velocity at the front and rear surfaces, and D_A – ambipolar diffusion coefficient. Then,

© 2019, V. Lashkaryov Institute of Semiconductor Physics, National Academy of Sciences of Ukraine

one can neglect the spatial non-uniformity of the excess carrier concentration, $\Delta n(x)$, where x is the coordinate perpendicular to the SC surface. This simplifies significantly the analysis of this SC-BC.

In the theoretical modeling of the SC-BC characteristics, the following recombination mechanisms in silicon are taken into account: Shockley–Read–Hall (SRH) recombination with the lifetime τ_{SRH}, non-radiative exciton Auger recombination assisted by deep impurities with the lifetime τ_{nr} [4], surface recombination on the front and rear surfaces with the respective velocities S_0 and S_d, radiative recombination with the lifetime τ_r [5], band-to-band Auger recombination [6], and the space-charge region (SCR) recombination with the velocity S_{SC}. In contrast to the traditional SCs, recombination on the front surface plays an important role in the SC-BC, so that the condition $S_0 << D_A/d$ may not always be fulfilled.

The theoretical dependence of the photoconversion efficiency η on the SC-BC base thickness d is obtained. Two mechanisms are operative in forming the short-circuit current dependence on the thickness. The first one accounts for the increase of the photon mean-free path in the textured SC-BC, and the second one is related to the effect of the recombination velocity on the illuminated surface, S_0.

The theoretical results are shown to be in good agreement with the experiment ones.

2. Effective recombination time in silicon

Taking all the above mentioned recombination mechanisms into account, the effective recombination time τ_{eff} in silicon is

$$\tau_{eff}(n) = \left[\frac{1}{\tau_{SRH}(n)} + \frac{1}{\tau_{nr}(n)} + \frac{S_{0S}}{d}\left(1 + \frac{\Delta n}{n_0}\right) + \frac{1}{\tau_r(n)} + \frac{1}{\tau_{Auger}(n)} + \frac{S_{SC}(n)}{d}\right]^{-1}, \quad (1)$$

where $n = n_0 + \Delta n$, n_0 is the equilibrium concentration of the majority carriers (assumed for definiteness to be electrons), $S_{0S} = S_{00} + S_{0d}$ – net (front plus rear) surface recombination velocity at low injection, $\tau_{nr}(n) = \tau_{SRH}\, n_x/n$ – non-radiative exciton recombination lifetime [4], $n_x = 8.2\cdot 10^{15}\,\text{cm}^{-3}$, $\tau_r(n)$ – radiative recombination lifetime [5], and $\tau_{Auger}(n)$ – Auger band-to-band recombination lifetime [6].

The SRH recombination lifetime τ_{SRH} in n-type silicon is given by the expression:

$$\tau_{SRH}(n) \cong \frac{\tau_{p0}\left(n_0 + \Delta n + n_1\right) + \tau_{n0}\left(p_1 + \Delta n\right)}{\left(n_0 + \Delta n\right)}, \quad (2)$$

where $\tau_{p0} = \left(C_p N_t\right)^{-1}$, $\tau_{n0} = \left(C_n N_t\right)^{-1}$, C_p and C_n are the capture coefficients for holes and electrons by a recombination center, N_t is the recombination center concentration, and n_1 and p_1 are the so-called SRH parameters, *i.e.*, the electron and hole concentrations in the case when the energy of the recombination level coincides with the Fermi energy.

Note that depending on the energy of the recombination center and the capture cross-sections for electrons and holes, the SRH lifetime as a function of the doping and the excitation level changes between two values and can increase, decrease, or remain practically constant in a certain range of the doping and excess concentrations. In what follows, we will consider the case when τ_{SRH} is constant within the range of doping and excess concentrations of interest, covering 10^{14} to $10^{16}\,\text{cm}^{-3}$.

For the radiative recombination lifetime $\tau_r(n)$ in silicon at $T = 300$ K, we will use the expression:

$$\frac{1}{\tau_r(n)} = A\left(n_0 + \Delta n\right), \quad (3)$$

where the radiative recombination parameter A was found in [5] taking into account both band-to-band and exciton radiative recombination and the results from [7]. It is given by

$$A \approx 6.3\cdot 10^{-15} \exp\left(-\frac{\Delta E_g(n_0 + \Delta n)}{kT}\right)\ \text{cm}^3/\text{s}, \quad (4)$$

where $\Delta E_g(n_0 + \Delta n)$ is the bandgap narrowing in silicon, found in [8].

With respect to the band-to-band Auger recombination lifetime, $\tau_{Auger}(n)$, we used the empirical expression from [6].

Recombination in the space-charge region in silicon is due to discreet impurities with the concentration N_t^* and the energy E_t close to the middle of the bandgap. These impurities can trap electrons and holes with the respective capture cross-sections σ_n and σ_p. When the SRH parameters n_1, p_1 are much smaller than the majority and minority concentrations, the analytical expression for the SCR recombination velocity is as follows [9, 10]:

$$S_{SC}(\Delta n) \approx \frac{kL_D e^{y_m}}{\tau_R\sqrt{\dfrac{(n_0 + \Delta n)(e^{-y_m} - 1) + (p_0 + \Delta n)(e^{y_m} - 1)}{n_0} + y_m}}. \quad (5)$$

Here, k is a numerical parameter of the order of unity, $y_m = (1/2)\ln\left((n_0 + \Delta n)/b_r\left(p_0 + \Delta n\right)\right)$ – dimensionless quantity that depends on the carrier concentrations and the ratio $b_r = \dfrac{\sigma_p\sqrt{m_e^*}}{\sigma_n\sqrt{m_h^*}}$ involving the charge carrier capture cross-sections and the effective masses,

$\tau_R = \left(\sigma_p v_p N_t^*\right)^{-1}$ – SRH lifetime in SCR, v_p – hole thermal velocity, N_t^* – recombination center concentration, n_0 and p_0 are the equilibrium electron and hole concentrations, $L_D = \left(\varepsilon_{Si} kT / 2q^2 n_0\right)^{1/2}$ – Debye length, ε_{Si} – dielectric constant of silicon, and q – elementary charge.

As shown in [9, 10], the value S_{SC} decreases with the excess electron-hole pair concentration Δn and with the SRH lifetime in SCR τ_R. In the direct-bandgap semiconductors, the SRH lifetime τ_{SRH} is small (see, *e.g.*, [11]), hence, the value S_{SC} can be quite high. SCR recombination can actually compete with the quasi-neutral bulk recombination even at those values of Δn that are characteristic for the maximal-power regime. Therefore, SCR recombination should be accounted in the SC modeling.

On the other hand, in the high-efficiency SC-BC, the bulk SRH lifetime, τ_{SRH}, is close to 10 ms [12], whereas the excess concentration Δn under maximal power conditions exceeds 10^{15} cm^{-3}. If we assume that $\tau_R \propto \tau_{SRH}$, then the SCR recombination velocity can be estimated as $S_{SC} \le 10^{-2}$ cm/s. At a first glance, SCR recombination can be neglected as compared to other recombination channels. However, as the analysis performed in [9, 10] shows, the main difference between the SCR and bulk recombination mechanisms is that the lifetime in SCR, τ_R, can be several orders of magnitude smaller than the SRH lifetime in the bulk, τ_{SRH}. For the cases analyzed in [9, 10], τ_R is close to 1 µs. In the first place, it means that the deep recombination center concentration in SCR is much higher than that in the neutral bulk. The reasons for this might be related to the gettering effect during the high-temperature diffusion in the *p-n* junction formation stage, the presence of boron complexes that promote an increase of the deep impurity concentration, the effects related to the high electric field in SCR, and possibly other mechanisms. As a result, the SCR recombination velocity in the high-efficiency SCs is also comparable with or even exceeds the recombination velocity of other recombination channels, meaning that it must be accounted for in the modeling of SC-BC as well.

3. Modeling the open-circuit voltage and short-circuit current in SC-BC

As shown in [13], the open-circuit voltage V_{OC} in silicon p^+-n-n^+ structures, including SC-BC, is given by the expression

$$V_{OC} \cong \frac{kT}{q} \ln\left(1 + \frac{\Delta n_{OC}}{p_0}\right) + \frac{kT}{q} \ln\left(1 + \frac{\Delta n_{OC}}{n_0}\right), \quad (6)$$

where Δn_{OC} is the excess concentration under the open-circuit conditions.

In SC-BC, the SCR recombination proceeds not uniformly in the whole SC area A_{SC}, but only in those regions, where an inversion band bending is created, that is, in the boron-doped regions. Their total area A_B is smaller than A_{SC}. Therefore, when the expression (1) is applied to SC-BC, one should replace the term S_{SC} with $S_{SC} \dfrac{A_B}{A_{SC}}$.

The *I-V* curve for illuminated SC-BC is calculated according to the expression [13]

$$I(V) = I_L - I_r(V - IR_S) + \frac{V - IR_s}{R_{SH}}, \quad (7)$$

where I_L is the photo-generated current, which equals the short-circuit current I_{SC} in the highly efficient SCs $I_L \approx \approx I_{SC}$, R_S and R_{SH} are the series and shunt resistances, and

$$I_r(V) = qA_{SC}\left(\frac{d}{\tau_{eff}^b} + S_{0S}\left(1 + \frac{\Delta n}{n_0}\right) + \frac{A_B}{A_{SC}} S_{sc}\right)\Delta n(V) \quad (8)$$

is the recombination current with the recombination lifetime in the base given by

$$\tau_{eff}^b(n) = \left[\frac{1}{\tau_{SRH}} + \frac{1}{\tau_r(n)} + \frac{1}{\tau_{nr}(n)} + \frac{1}{\tau_{Auger}(n)}\right]^{-1} \quad (9)$$

and the excess concentration found from the expression

$$\Delta n(V) = -\frac{n_0 + p_0}{2} + \sqrt{\frac{(n_0 + p_0)^2}{4} + n_i(T, \Delta E_g)^2\left(\exp\frac{q(V - IR_s)}{kT} - 1\right)}. \quad (10)$$

Here, $p_0 = n_i^2(T, \Delta E_g)/n_0 = n_{i0}^2(T)\exp(\Delta E_g / kT)/n_0$ is the equilibrium hole concentration in the *n*-type base, $\Delta E_g(n_0 + \Delta n)$ – bandgap narrowing in silicon, determined in the work [8], and $n_{i0}(T)$ – intrinsic charge carrier concentration without band narrowing [7]. The latter expression (10) immediately follows from the uniformity of the excess concentration profile within the base, implying that the difference between the electron and hole quasi-Fermi energies equals to the voltage across the base times the elementary charge. This voltage is given by the difference between the applied voltage and voltage drop on the series resistance, $V - IR_S$. Then, the product of non-equilibrium electron and hole concentrations obeys the relationship $(p_0 + \Delta n)(n_0 + \Delta n) = n_i^2 e^{q(V - IR_S)/kT}$, which can be solved for Δn, giving (10).

Multiplying the current $I(V)$ by the applied voltage V, we obtain the power $P(V)$. From the maximum power condition $d[P(V)]/dV = 0$, we find the voltage V_m at the maximal power. Substitution of V_m into (8) gives the respective current I_m, which allows one to determine the photoconversion efficiency $\eta = I_m V_m / (A_{SC} P_{light})$ and the

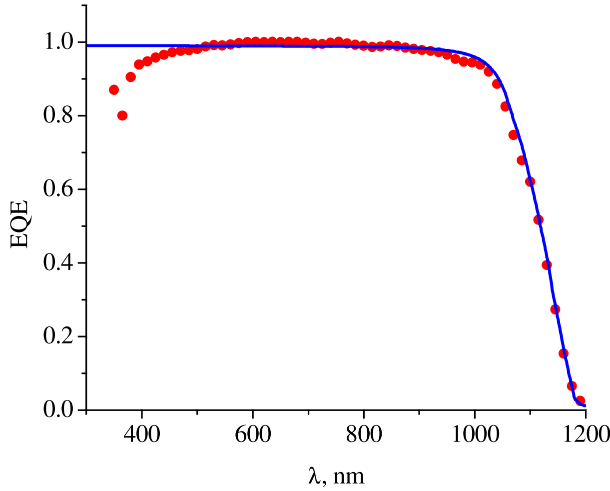

Fig. 1. Experimental (symbols) and theoretical (solid line) external quantum efficiency for the SCs from [15].

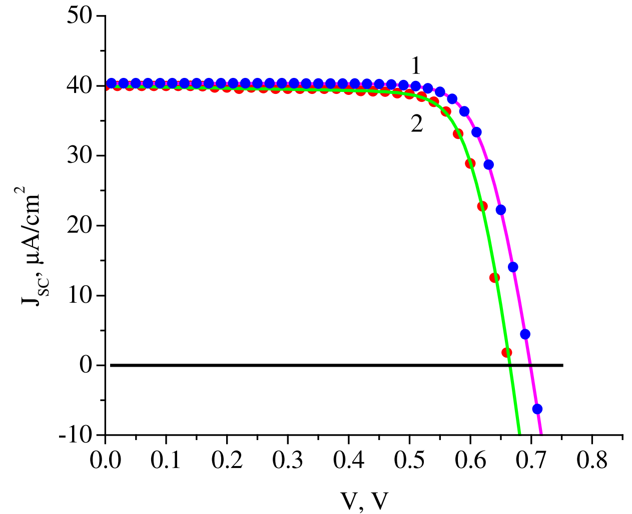

Fig. 3. Experimental (symbols) and theoretical (solid lines) *I-V* curves of the illuminated commercial SCs by SunPower (*1*) and the *I-V* curves for the illuminated SC from [15] (*2*).

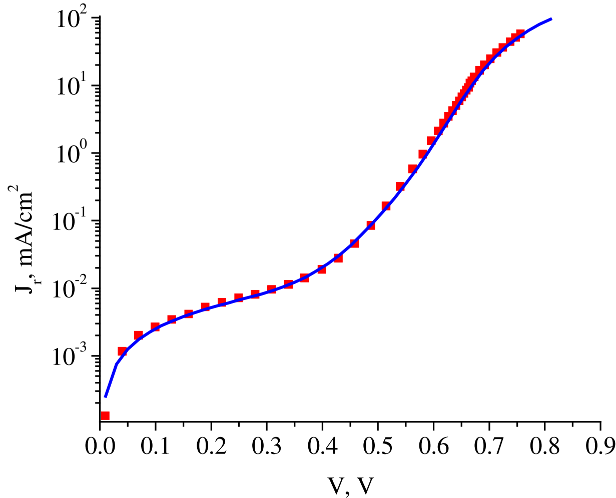

Fig. 2. Experimental (symbols) and theoretical (solid line) dark *I-V* curves of the commercial SCs by SunPower.

fill factor $FF = I_m V_m / (I_{SC} V_{OC})$, where P_{light} is the incident irradiance, equal to 0.1004 W/cm² for the AM1.5 conditions.

The short-circuit current is a parameter that should be determined experimentally. On the other hand, in the textured SCs it can be calculated, if one knows the external quantum efficiency of the photogenerated current $EQE(\lambda)$. As shown in the work [14], the external quantum efficiency *EQE* in a textured *p-n* junction-based silicon SCs, as well as in a heterojunction SCs, is described in the long-wave region by an empirical expression

$$EQE(\lambda, b) = \left(1 + \frac{b}{4\alpha(\lambda) d n_r^2}\right)^{-1}, \qquad (11)$$

where *b* is a numerical coefficient exceeding the unity. Here, it is assumed that in the long-wave region, the external quantum efficiency is approximately the same as the internal quantum efficiency $EQE(\lambda,b) = T(\lambda)\cdot IQE(\lambda,b) \approx IQE(\lambda,b)$, because the transmission coefficient $T(\lambda)$ in this part of the spectrum is close to unity.

Shown in Fig. 1 are the experimental curves $EQE(\lambda)$ for SC-BC from [15] and their approximation by the expression (11). The coefficient *b*, at which the theory agrees well with the experiment in the long-wave region, equals 1.6. As seen in Fig. 1, the expression (11) quite accurately describes $EQE(\lambda)$ within the wavelength range from 800 up to 1200 nm. Hence, for this SC-BC one can determine

$$J_{SC}(d,b) = q\left[\int_{\lambda_0}^{800} I_{AM1.5}(\lambda) EQE(\lambda) d\lambda + f\int_{800}^{\lambda_m} I_{AM1.5}(\lambda) EQE(\lambda,b) d\lambda\right], \qquad (12)$$

where $\lambda_0 = 300$ nm, $\lambda_m = 1200$ nm, $I_{AM1.5}(\lambda)$ is the spectral photon flux under the AM1.5 conditions, $EQE(\lambda,b)$ is given by (12), and the coefficient $f \le 1$ should be chosen in such a manner that for $\lambda = 800$ nm the values $EQE(\lambda)$ and $IQE(\lambda,b)$ are the same.

4. Results and discussion

In order to model SC-BC, one needs to determine the recombination parameters τ_R and b_r. They can be found from the dark *I-V* curves. Because we could not find the dark *I-V* curves in literature for these SCs (see, *e.g.*, [15, 16]), just the illuminated ones, we have measured them

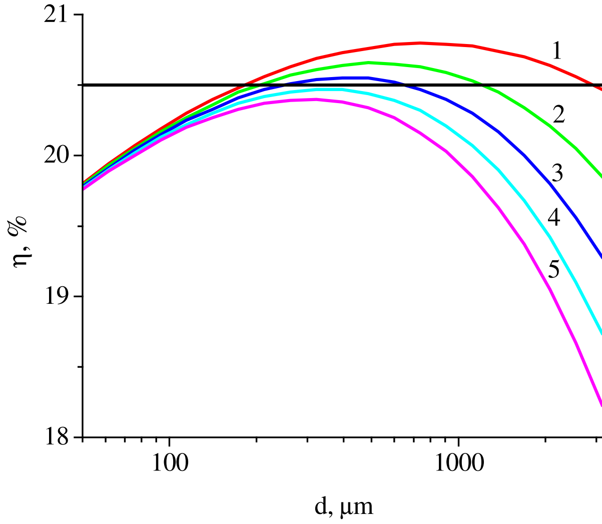

Fig. 4. Thickness dependence of the photoconversion efficiency η(*d*) for SCs from [15]. The curves *1* to *5* correspond to S_{00} = 0, 1, 2, 3, and 4 cm/s, respectively.

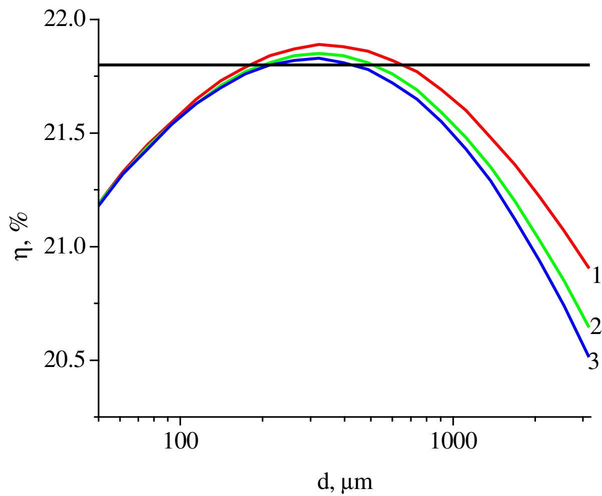

Fig. 5. Thickness dependence of the photoconversion efficiency for SC by SunPower. The curves *1–3* are plotted for S_{00} = 0, 0.4, and 0.6 cm/s, respectively.

on some commercial SC-BC with the area A_{SC} = 153 cm^2 and the base thickness d = 165 μm. The experimental dark current density $J_r(V)$ shown in Fig. 2 was fitted by the theoretical expressions above. In the modeling, the SRH recombination lifetime was taken to be τ_{SRH} = = 10 ms, which is consistent with [16]. As a result of this fitting, the following parameters have been obtained: the net surface recombination velocity at low injection S_{0S} = 4 cm/s, the SCR recombination lifetime τ_R = 20 μs, the ratio of the electron to hole capture coefficients $b_r = 2\cdot10^{-2}$.

Fig. 3 shows the *I-V* curve for illumination conditions, which was measured by us under the AM1.5 conditions by using commercial SC-BC, as well as the *I-V* curve from [15]. As seen in this figure, the open-circuit voltage V_{OC} = 0.698 V for the commercial SC, and for the SC sample from [15] it equals 0.655 V. The short-circuit current density J_{SC} of the commercial SC is 40.04 mA/cm^2, and for that from [15] it is 40 mA/cm^2.

By applying the theory to fit the experimental *I-V* curves under illumination, one can determine several parameters of these SC-BC, namely: the surface recombination velocity S_{0S} and parasitic specific resistances R_s and R_{sh}. The value of S_{0S} in SCs from [15] turned out to be 16 cm/s, whereas for the commercial SC it was 4 cm/s, which coincides with the value obtained from fitting the dark *I-V* curve of this SC-BC. By fitting the illuminated *I-V* curves, also the products of the specific series and shunt resistances and the SC area, AR_s and AR_{sh}, were found to be, respectively, 1.22 and $4\cdot10^4$ Ω·cm^2 for the commercial SC-BC and 1 and $7\cdot10^2$ Ω·cm^2 for SC from [15].

Having the relationship (13) between the photogenerated current and the base thickness, $J_L(d)$, and the parameters found from fitting the illuminated *I-V* curves, one can determine how the photoconversion efficiency depends on the base thickness. For SC from [15], the respective curve is shown in Fig. 4, curve *1*. When plotting this curve, it was assumed that the τ_R and b_r values are, respectively, 20 μs and $2\cdot10^{-2}$. As seen in Fig. 4, the optimal thickness d_{opt} equals 738 μm, which is significantly higher than the experimental base thicknesses used in SC-BC. Such a high value of d_{opt} in this case is due to the high net surface recombination velocity at low injection, S_{0S}.

It should be noted that the obtained result is valid only if the criterion $S_0 d/D_A \ll 1$ is fulfilled. It is well-known (see, *e.g.*, [17, 18]) that surface recombination on the front (illuminated) surface of silicon SC-BC decreases the short-circuit current density J_{SC} according to

$$J_{SC} = \frac{J_{SC0}}{1 + \dfrac{S_0(\Delta n)\, d}{D_A(\Delta n)}}, \qquad (13)$$

where $J_{SC0} = J_{SC}(d, b)$,

$$D_A(\Delta n) = \frac{n_0 + p_0 + 2\Delta n}{\dfrac{n_0 + \Delta n}{D_p(\Delta n)} + \dfrac{p_0 + \Delta n}{D_n(\Delta n)}} \qquad (14)$$

is the ambipolar diffusion coefficient, $D_p(\Delta n)$ and $D_n(\Delta n)$ are the hole and electron diffusion coefficients, which are related to the respective mobilities in accord with Einstein's relation.

We are analyzing the case of *n*-type doping, *i.e.* $n_0 \gg p_0$. We also consider the general case when the excess carrier concentration Δn is not bounded from above and may exceed the equilibrium majority concentration n_0.

Let us evaluate the effect of the surface recombination velocity S_0 and base thickness d on the photoconversion efficiency in SC-BC. Strictly speaking, the values of

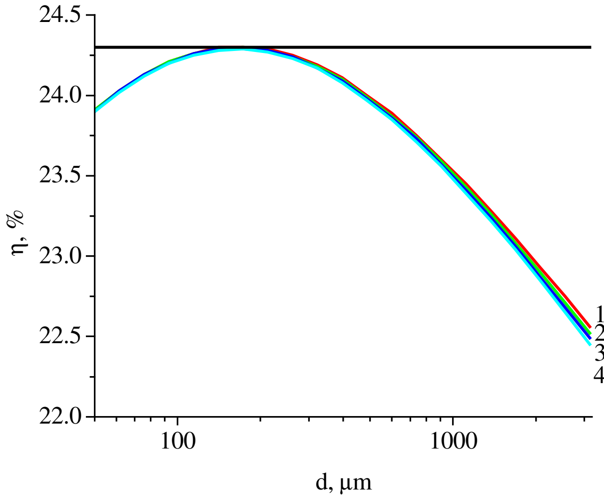

Fig. 6. Thickness dependence of η(*d*) for SCs from [16]. The curves *1* to *4* correspond to S_{00} = 0, 0.06, 0.1, and 0.15 cm/s, respectively.

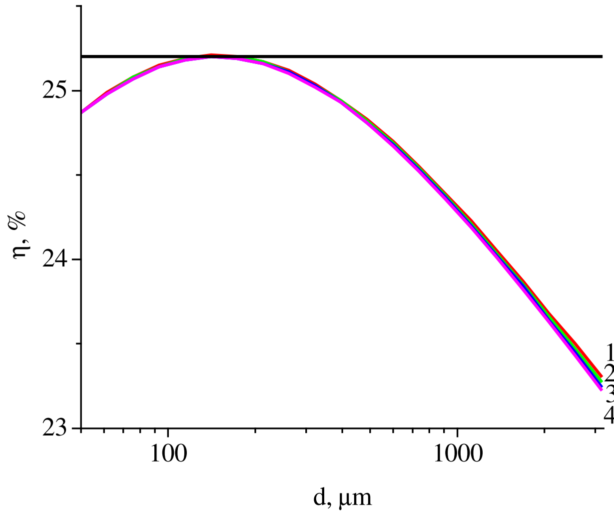

Fig. 7. Thickness dependence η(*d*) for SCs from [2]. The curves *1* to *4* are obtained for S_{00} = 0, 0.04, 0.07 and 0.1 cm/s, respectively.

D_p and D_n are not fixed when $\Delta n \geq n_0$. To simplify the analysis, let us consider the situation when D_p and D_n have their low-injection values, D_{p0} = 11.25 cm^2/s and D_{n0} = 33.75 cm^2/s, and the resistivity of silicon is sufficiently high. We also take into account that $S_0(\Delta n) = S_{00}(1 + \Delta n/n_0)$, where S_{00} is the low-injection recombination velocity on the front surface. Then, the expression (14) takes the form

$$J_{SC} = \frac{J_{SC}(d,b)}{1 + S_{00}\left(1 + \frac{\Delta n}{n_0}\right) d \frac{\frac{n_0 + \Delta n}{D_{p0}} + \frac{\Delta n}{D_{n0}}}{n_0 + 2\Delta n}}. \quad (15)$$

Fig. 4 also shows the photoconversion efficiency η as a function of the base thickness *d* for SCs from [15] obtained using the expression (15). The total front and rear surface recombination velocity at low injection S_{0S} was taken to be 16 cm/s. The curves *2–5* correspond to the low-injection front surface recombination velocity S_{00} equal to 1, 2, 3, and 4 cm/s, whereas for each curve, the rear surface recombination velocity was taken as $S_{0S} - S_{00}$. This had practically no effect on the open-circuit voltage. As seen in the figure, increasing S_{00} results in a decrease of both maximal efficiency η_m and the optimal base thickness d_{opt}, for which η is maximal. The highest value of d_{opt} is about 738 μm, whereas the minimal value is 320 μm. But at the typical SC-BC thickness of 150 μm, the reduction of η is relatively small, being of the order of 0.7%.

Because this result is caused by the high value of S_{0S} in SC-BC from [15], let us analyze the effect of recombination velocity at the front surface for commercial SC, which *I-V* curve for illumination conditions is also presented in Fig. 2. For this SC, the value S_{0S} = 4 cm/s, which is 4 times as low as for SC from [15]. Accordingly, the value of S_{00} is also lower. Fig. 5 shows the theoretical photoconversion efficiency η(*d*) for the commercial SC-BC, obtained using the same calculation scheme as in the previous case, but with S_{0S} = = 4 cm/s. The curve *1* is obtained under the assumption that surface recombination velocity does not affect the short-circuit current, whereas the curves *2* and *3* correspond to the low-injection front surface recombination velocity S_{00} of 0.4 and 0.6 cm/s. As seen from Figs. 4 and 5, the tested commercial SC is characterized by a smaller drop in both the maximal efficiency and the optimal thickness as S_{00} is increased. The maximal η-value is 21.8%, which differs by only 0.5% from the efficiency at *d* = 165 μm. The initial optimal thickness d_{opt} is about 322 μm, which is also lower than for SC from [15].

Ref. [16] gives the key parameters of high-efficiency SC-BC produced by the company SunPower. The highest photoconversion efficiency is 24.3%, and the open-circuit voltage is 0.730 V. Assuming that in this SC τ_{SRH} = 10 ms, as before, the doping level of $9\cdot10^{14}$ cm^{-3}, and τ_R = 20 μs and $b_r = 2\cdot10^{-2}$, we determined the thickness dependence of the photoconversion efficiency η(*d*) for this SC-BC. First, from fitting the experimental open-circuit voltage V_{OC}, the value of S_{0S} was found to be 0.6 cm/s. Then, from a comparison between the theoretical and experimental η-values at the thickness 150 μm, the specific resistance value AR_s = 0.26 Ω·cm^2 was determined. After that, the curves η(*d*) were plotted and shown in Fig. 6 (curve *1*). As seen in the figure, the maximal η is 24.3% at the optimal thickness d_{opt} = 173 μm. The curves *2* to *4* are obtained for the low-injection front surface recombination velocity S_{00} equal to 0.06, 0.1 and 0.15 cm/s, respectively. Again, the values of efficiency η at *d* = 173 μm are practically the same at different values of S_{00}. That is, $S_0 d/D_A \leq 0.001$.

Finally, shown in Fig. 7 are the efficiency *vs* base thickness curves for SC-BC with the record efficiency of 25.2% from Ref. [2]. The following parameter values were assumed: τ_{SRH} = 10 ms, doping level $9\cdot10^{14}$ cm^{-3}, τ_R = 20 µs and $b_r = 2\cdot10^{-2}$. From fitting the experimental open-circuit voltage with the theory, it was found that S_{0S} = 0.42 cm/s. Then, but comparing the theoretical and experimental efficiency at the thickness 130 µm, the specific series resistance value of AR_s = 0.25 Ω·cm^2 was found. Finally, the curves η(*d*) were plotted, see Fig. 7 (curve *1*). As seen in this figure, the maximal efficiency has the value of 25.2% at the optimal thickness d_{opt} = = 141 µm. The curves *2* to *4* correspond to the low-injection front surface recombination velocity S_{00} of 0.04, 0.07 and 0.1 cm/s, respectively. Again, as in the previous case, the efficiency values at *d* = 141 µm are practically the same at different S_{00}. That is, $S_0 d/D_A \le 10^{-4}$.

Comparison of Figs. 6 and 7 indicates that as the photoconversion efficiency in SC-BC increases, the optimal thickness d_{opt} slightly decreases.

5. Conclusions

The results of our analysis show that two mechanisms are operative in the thickness dependence of the photoconversion efficiency in SC-BC. The first one is related to an increase of the photon mean free path in textured SCs and is the more pronounced the smaller is the value of the parameter *b* in the expression (12). The other mechanism has to do with the recombination velocity on the front surface. The effect of surface recombination on the illuminated surface on the short-circuit current in the analyzed SC-BC is the smaller the lower is the net surface recombination velocity at the front and rear surfaces. Besides, the value of S_0 is always smaller than S_d, which is taken into account in the calculations. The open-circuit voltage is affected only by the total front and rear surface recombination velocity S_S.

The higher S_S, the larger the optimal base thickness d_{opt} at which the photoconversion efficiency is maximal, and the bigger the shift of d_{opt} to the smaller values in the case when S_0 is increased. At the same time, the curves η(*d*) in the thickness range between 150 and 800 µm in the silicon SC-BC produced by SunPower are rather flat, hence using the thickness of (150 ± 30) µm does not lead to a significant reduction of the efficiency as compared to the maximal values.

References

1. Battaglia C., Cuevas A., and De Wolf S. High-efficiency crystalline silicon solar cells: Status and perspectives. *Energy Environ. Sci.* 2016. **9**. P. 1552–1576. https://doi.org/10.1039/C5EE03380B.
2. Smith D.D., Reich G., Baldrias M. *et al.* Silicon solar cells with total area efficiency above 25%. *2016 IEEE 43rd Photovoltaic Specialists Conference* (PVSC). P. 3351–3355.
3. https://us.sunpower.com/sites/default/files/media-library/data-sheets/ds-x21-series-335-345-residential-solar-panels.pdf.
4. Sachenko A.V., Kostylyov V.P., Vlasyuk V.M. *et al.* The influence of the exciton nonradiative recombination in silicon on the photoconversion efficiency. *Proc. 32 European Photovoltaic Solar Energy Conf. and Exhib.* Germany, Munich, June 20-24, 2016. P. 141–147.
5. Sachenko A.V., Gorban A.P., Kostylyov V.P. *et al.* The radiative recombination coefficient and the internal quantum yield of electroluminescence in silicon. *Semiconductors*. 2006. **40**, No 8. P. 884–889. https://doi.org/10.1134/S1063782606080045.
6. Richter A., Glunz S., Werner F. *et al.* Improved quantitative description of Auger recombination in crystalline silicon. *Phys. Rev. B.* 2012. **86**. P. 165202(1–14). https://doi.org/10.1103/PhysRevB.86.165202.
7. Trupke T., Green M.A., Wurfel P. *et al.* Temperature dependence of the radiative recombination coefficient of intrinsic crystalline silicon. *J. Appl. Phys*. 2003. **94**, No 8. P. 4930–4937. https://doi.org/10.1063/1.1610231.
8. Schenk A. Finite-temperature full random-phase approximation mode of band gap narrowing for silicon device simulation. *J. Appl. Phys*. 1998. **84**, No 7. P. 3684–3695. https://doi.org/10.1063/1.368545.
9. Kostylyov V.P., Sachenko A.V., Sokolovskyi I.O. *et al.* Influence of surface centers on the effective surface recombination rate and the parameters of silicon solar cells. *Ukr. J. Phys.* 2013. **58**, No 4. P. 362–369.
10. Sachenko A.V., Kostylyov V.P., Sokolovskyi I.O. *et al.* Specific features of current flow in α-Si : H/Si heterojunction solar cells. *Techn. Phys. Lett.* 2017. **43**, No 2. P. 152–155. https://doi.org/10.1134/S1063785017020109.
11. Sachenko A.V., Kostylyov V.P., Kulish N.R. *et al.* Modeling the efficiency of multijunction solar cells. *Semiconductors.* 2014. **48**, No 5. P. 675–682. https://doi.org/10.1134/S1063782614050182.
12. Verlinden P.J., Chapter IC-5 – High-Efficiency Back-Contact Silicon Solar Cells for One-Sun and Concentrator Applications, in: *Solar Cells* (Second Edition), Materials, Manufacture and Operation. Elsevier, 2013. P. 327–351. https://doi.org/10.1016/B978-0-12-386964-7.00011-1.
13. Gorban A.P., Sachenko A.V., Kostylyov V.P., Prima N.A. Effect of excitons on photoconversion efficiency in the p^+-n-n^+- and n^+-p-p^+-structures based on single-crystalline silicon. *Semiconductor Physics, Quantum Electronics & Optoelectronics.* 2000. **3**, No 3. P. 322–329; Sachenko A.V., Prima N.A., Gorban A.P., Serba A.A. Effect of excitons on the upper limit of conversion efficiency in silicon solar cells. *Proc. 17-th European Photovoltaic Solar Energy Conference*. Munich, Germany, 2001. P. 230–233.

14. Sachenko A.V., Kostylyov V.P., Bobyl A.V. *et al.* The effect of base thickness on photoconversion efficiency in textured silicon-based solar cells. *Techn. Phys. Lett.* 2018. **44**, No 10. P. 873–876. https://doi.org/10.1134/S1063785018100139.
15. http://eshop.terms.eu/_data/s_3386/files/1379942540-sunpower_c60_bin_ghi.pdf.
16. https://us.sunpower.com/sites/default/files/media-library/spec-sheets/sp-sunpower-maxeon-solar-cells-gen3.pdf.
17. Sachenko A.V., Gorban A.P., Kostylyov V.P. *et al.* The specific features of photoconversion in Si solar cells for the standard and rear contact positions under concentrated illumination. *Ukr. J. Phys*. 2007. **52**, No 7. P. 661–670; Sachenko A.V., Gorban A.P., Kostylyov V.P. *et al.* Comparative analysis of photoconversion efficiency in the Si solar cells under concentrated illumination for the standard and rear geometries of arrangement of contacts. *Semiconductors.* 2007. **41**, No 10. P. 1214–1223. https://doi.org/10.1134/S106378260710017X.
18. Swanson R.M. Point-contact solar cells: Modeling and experiment. *Solar Cells.* 1986. **17**, No 1. P. 85–118. https://doi.org/10.1016/0379-6787(86)90061-X.

Authors and CV

Sachenko A.V., Professor, Doctor of Physics and Mathematics Sciences, Chief Researcher of the Laboratory of Physical and Technical Fundamentals of Semiconductor Photovoltaics at the V. Lashkaryov Institute of Semiconductor Physics. He is the author of more than 294 scientific publications. His main research interests include analysis, characterization, and modelling of silicon solar cells.

Kostylyov V.P., Doctor of Physics and Mathematics Sciences, Head of the Laboratory of Physical and Technical Fundamentals of Semiconductor Photovoltaics at the V. Lashkaryov Institute of Semiconductor Physics. He is the author of more than 250 scientific publications. The area of his scientific interests includes development of equipment for silicon solar cells testing, research, analysis of silicon solar cells.

Vlasyuk V.M., PhD, Researcher of the Laboratory of Physical and Technical Fundamentals of Semiconductor Photovoltaics at the V. Lashkaryov Institute of Semiconductor Physics. He is the author of more than 35 scientific publications. The area of his scientific interests includes research, analysis of silicon solar cells.

Korkishko R.M., PhD, Researcher of the Laboratory of Physical and Technical Fundamentals of Semiconductor Photovoltaics at the V. Lashkaryov Institute of Semiconductor Physics. He is the author of more than 46 scientific publications. The area of his scientific interests includes research, analysis of silicon solar cells.

Sokolovskyi I.O., Senior Researcher of the Laboratory of Physical and Technical Fundamentals of Semiconductor Photovoltaics at the V. Lashkaryov Institute of Semiconductor Physics. His main research interests include modelling of silicon solar cells.

Chernenko V.V., Senior Researcher of the Laboratory of Physical and Technical Fundamentals of Semiconductor Photovoltaics at the V. Lashkaryov Institute of Semiconductor Physics. He is the author of more than 100 scientific publications. His main research interests include research, analysis of silicon solar cells.

Dvernikov B.F., Researcher of the Laboratory of Physical and Technical Fundamentals of Semiconductor Photovoltaics at the V. Lashkaryov Institute of Semiconductor Physics. The area of his scientific interests includes manufacturing of equipment for silicon solar cells testing.

Serba O.A., Leading Researcher of the Laboratory of Physical and Technical Fundamentals of Semiconductor Photovoltaics at the V. Lashkaryov Institute of Semiconductor Physics. He is the author of more than 120 scientific publications. His research areas are the research, analysis of silicon solar cells.

Evstigneev M.A., Assistant Professor of the faculty of Physics and Physical Oceanography at the Memorial University of Newfoundland. His research areas are non-equilibrium statistical physics, biophysics, surface science.